Supporting Information

Cu Electrodeposition on Nanostructured MoS_2 and WS_2 and Implications for HER Active Sites Determination

[1]Longfei Wu, [2, 3]Nelson Y. Dzade, [4]Ning Chen, [5]Bas van Dijk, [6]Shashank Balasubramanyam, [6]Akhil Sharma, [1]Lu Gao, [5]Dennis G. H. Hetterscheid, [1]Emiel J. M. Hensen, [6]Ageeth A. Bol, [2, 7]Nora H. De Leeuw, [1, 8 z]Jan P. Hofmann

[1]*Laboratory for Inorganic Materials and Catalysis, Department of Chemical Engineering and Chemistry, Eindhoven University of Technology, P.O. Box 513, 5600 MB Eindhoven, The Netherlands*
[2]*Faculty of Geosciences, Utrecht University, P.O. Box 80.021, 3508 TA Utrecht, The Netherlands*
[3]*School of Chemistry, Cardiff University, Main Building, Park Place, CF10 3AT, Cardiff, United Kingdom*
[4]*Hard X-Ray MicroAnalysis (HXMA) BL, Canadian Light Source, University of Saskatchewan, 44 Innovation Boulevard, Saskatoon, SK, S7N 2V3, Canada*
[5]*Leiden Institute of Chemistry, Leiden University, Einsteinweg 55, 2333 CC Leiden, The Netherlands*
[6]*Department of Applied Physics, Eindhoven University of Technology, P.O. Box 513, 5600 MB Eindhoven, The Netherlands*
[7]*School of Chemistry, University of Leeds, Leeds LS2 9JT, United Kingdom*
[8] *Surface Science Laboratory, Department of Materials and Earth Sciences, Technical University of Darmstadt, Otto-Berndt-Strasse 3, 64287 Darmstadt, Germany*

[z]Corresponding author e-mail address [hofmann@surface.tu-darmstadt.de (JPH)]

TABLE OF CONTENTS

Part I: Cu underpotential deposition (UPD)

All Cu UPD tests were performed in Ar sturated 2 mM $CuSO_4$ in 0.1 M H_2SO_4 electrolyte. Briefly, the samples were firstly polarized at +0.67 V vs. RHE for 120 s to remove surface oxide species, then copper or hydrogen deposition was carried out at the indicated potential for 100 s. Afterwards, the potential was scanned to +0.67 V vs. RHE (lower potential could not fully strip Cu on MoS_2 and higher potential would cause oxidation of MoS_2) at a scan rate of 2 mV/s. Background hydrogen adsorption charge Q_{BC} was calculated by integrating the current obtained upon scanning from the deposition potential to +0.67 V vs. RHE. The Cu stripping charge Q_{Cu} was calculated in a similar way with correction for background hydrogen adsorption charge.

Table S1. Summary of the Cu stripping charge and background hydrogen adsorption charge at different potentials for nanostructured MoS_2.

Potential vs. RHE (V)	Q_{BC} (μC/cm^2)	Q_{Cu} (μC/cm^2)	Q_{Cu}/Q_{BC}
+0.33	54.6	290.2	5.3
+0.36	42.7	237.7	5.6
+0.39	31.3	166.2	5.3
+0.41	24.0	105.7	4.4
+0.44	16.3	41.1	2.5
+0.47	11.0	9.4	0.8
+0.50	7.5	3.5	0.5
+0.53	5.8	1.4	0.2
+0.55	4.8	0.2	0.1
+0.60	5.3	2.5	0.5

Table S2. Summary of the Cu stripping charge and background hydrogen adsorption charge at different potentials for WS_2 film.

Potential vs. RHE (V)	Q_{BC} (μC/cm^2)	Q_{Cu} (μC/cm^2)	Q_{Cu}/Q_{BC}
+0.335	38.9	282.0	7.2
+0.355	35.0	249.1	7.1
+0.385	27.7	217.3	7.8
+0.415	23.7	171.4	7.2
+0.435	20.3	121.6	6.0
+0.455	17.1	59.2	3.5
+0.465	15.7	28.1	1.8
+0.475	14.2	8.6	0.6
+0.485	13.0	4.0	0.3
+0.495	11.8	2.9	0.2
+0.505	10.6	2.2	0.2
+0.535	7.6	0.9	0.1
+0.565	5.3	0.6	0.1
+0.595	3.7	1.1	0.3

Part II: Comparison between Cu UPD and C_{dl}

Table S3. Summary of sample codes and corresponding ALD cycles and structures.

Sample codes	ALD cycles	Morphology
WS_2-1	200	Edge-enriched
WS_2-2	200	out-of plane oriented (OoPO)(1)
WS_2-3	400	Edge-enriched
WS_2-4	400	OoPO
WS_2-5	100	Edge-enriched
WS_2-6	600	Edge-enriched
MoS_2-1	100	OoPO(1, 2)
MoS_2-2	400	OoPO
MoS_2-3	600	OoPO
MoS_2-4	400	Amorphous

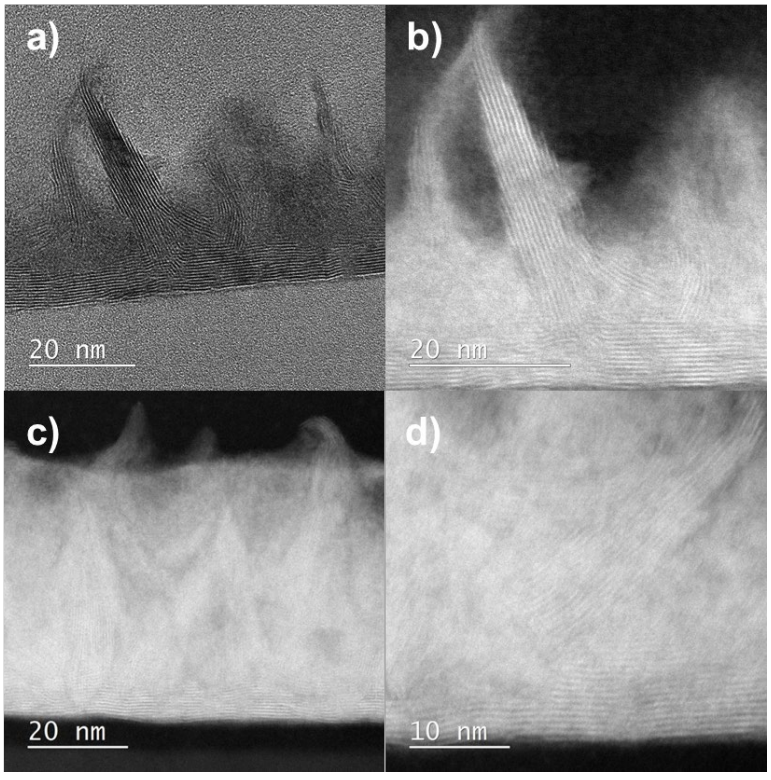

Fig. S1. Cross-section TEM (a) and HAADF-STEM (b) image of MoS_2 OoPO film; c, d) HAADF-STEM images of edge-enriched WS_2 films. Figures adapted with permission from: a,b ref. 2, Royal Society of Chemistry (2018) and c–d ref. 1, American Chemical Society (2019).

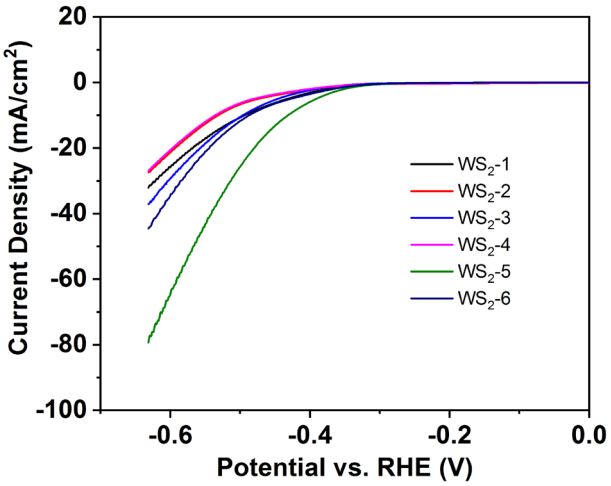

Fig. S2. Linear sweep voltammetry (LSV) curves of different WS_2 films in 0.1 M H_2SO_4. Scan rate: 5 mV/s.

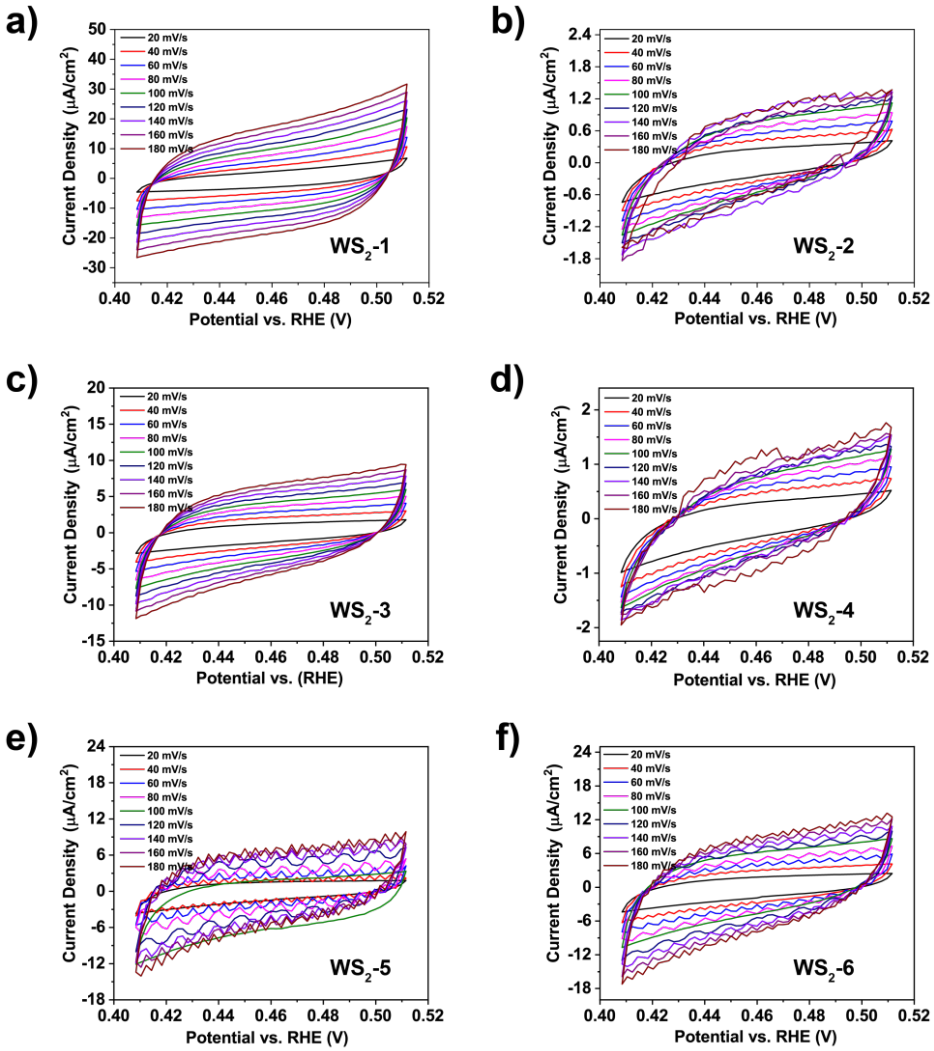

Fig. S3. a-f) Cyclic voltammetry (CV) measurements of different WS_2 films.

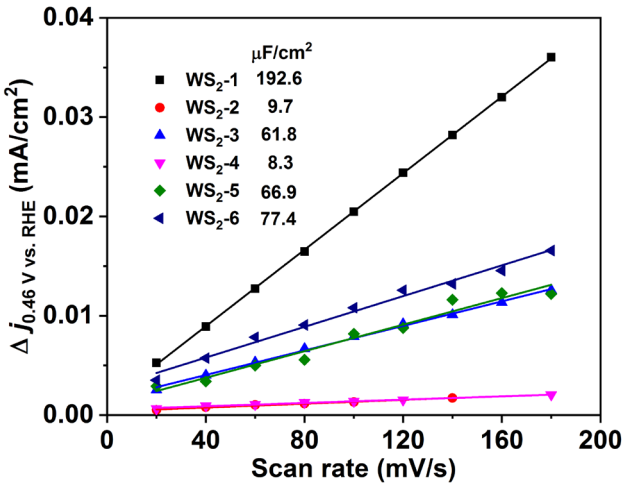

Fig. S4. Fitting plots showing the extraction of the corresponding C_{dl} from Fig. S4.

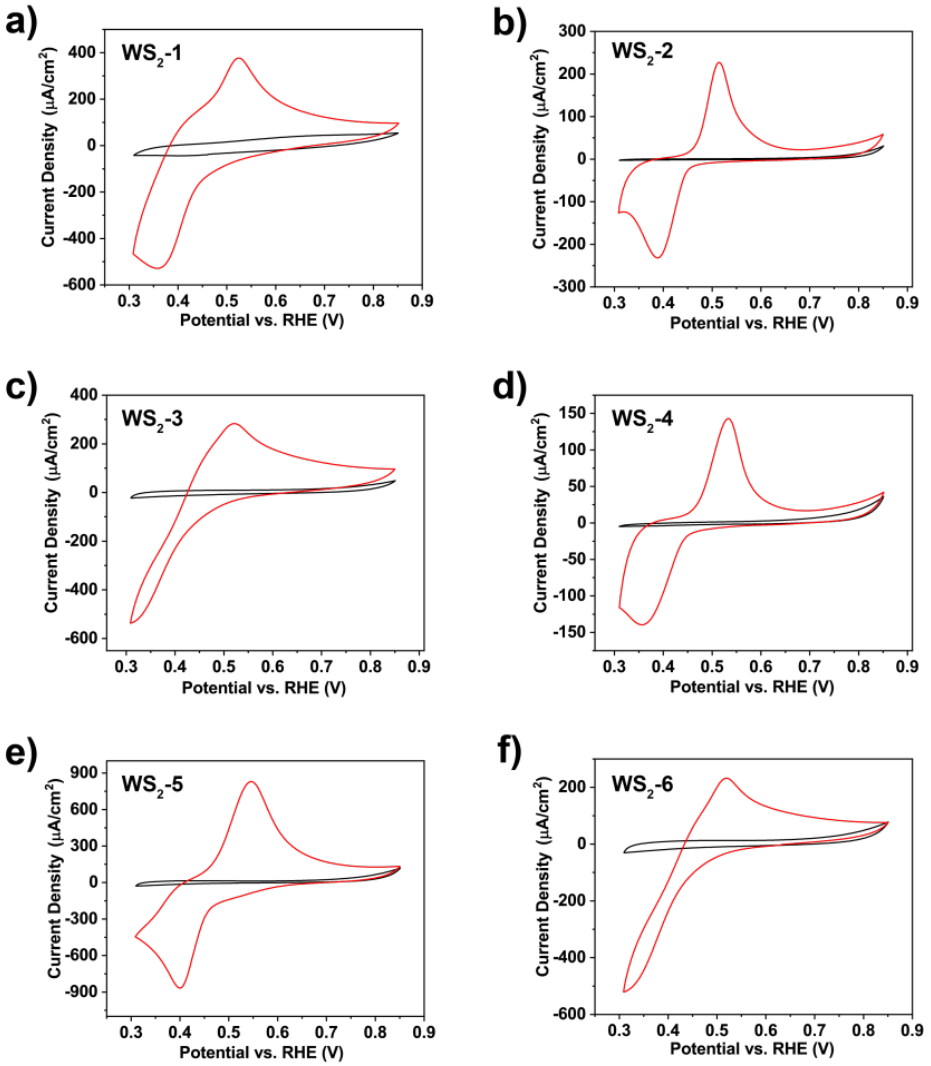

Fig. S5. CV tests for corresponding WS_2 films in 0.1 M H_2SO_4 (black curve) and in 2 mM $CuSO_4$ in 0.1 M H_2SO_4 (red curve).

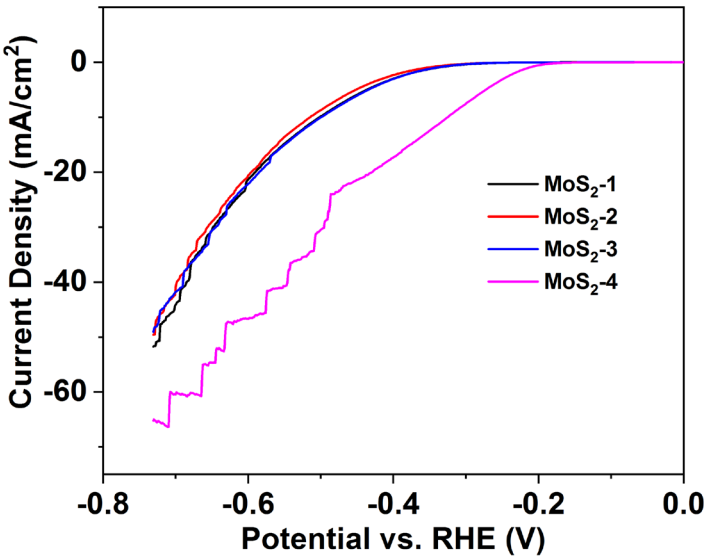

Fig. S6. Linear sweep voltammetry (LSV) curves of different MoS_2 films in 0.1 M H_2SO_4. Scan rate: 5 mV/s.

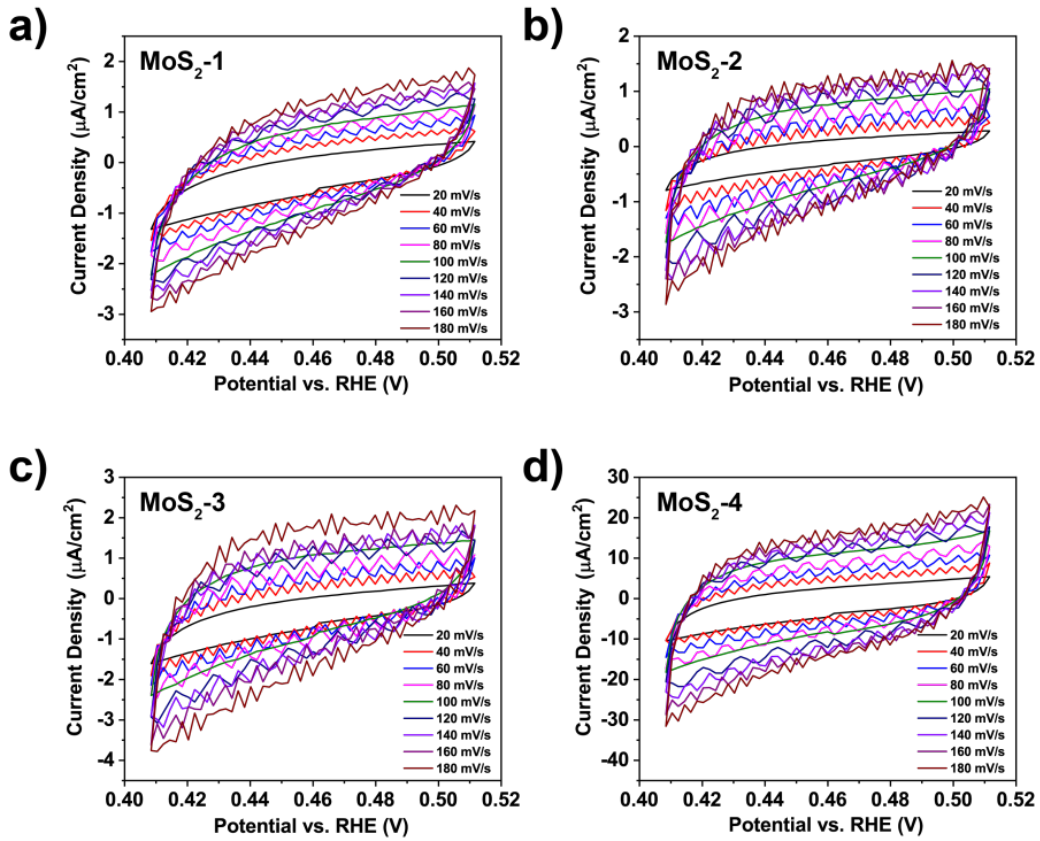

Fig. S7. a-d) Cyclic voltammetry (CV) measurements of different MoS_2 films.

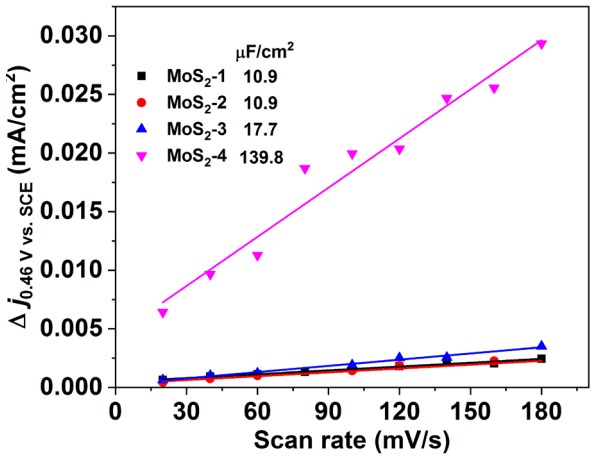

Fig. S8. Fitting plots showing the extraction of the corresponding electrochemical double layer capacitance (C_{dl}) from Fig. S8.

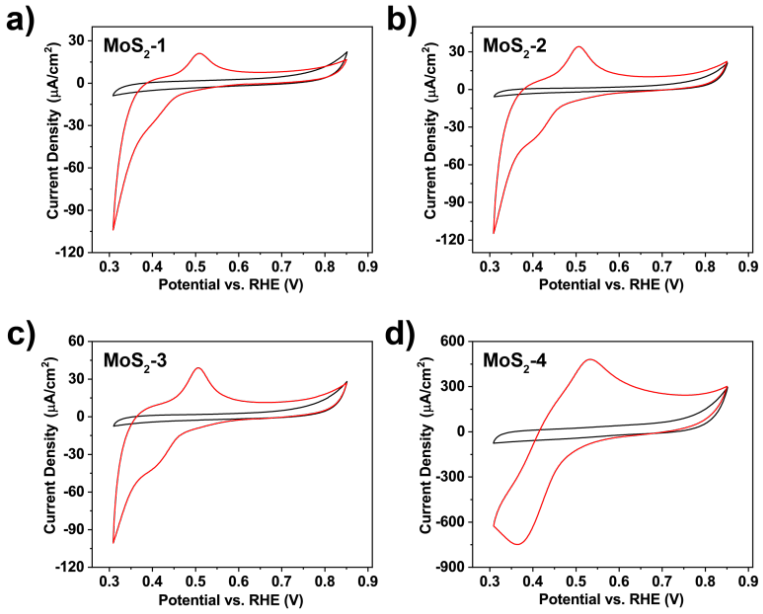

Fig. S9. CV tests for corresponding MoS_2 films in 0.1 M H_2SO_4 (black curve) and in 2 mM $CuSO_4$ in 0.1 M H_2SO_4 (red curve).

Part III: X-ray absorption spectroscopy (XAS)

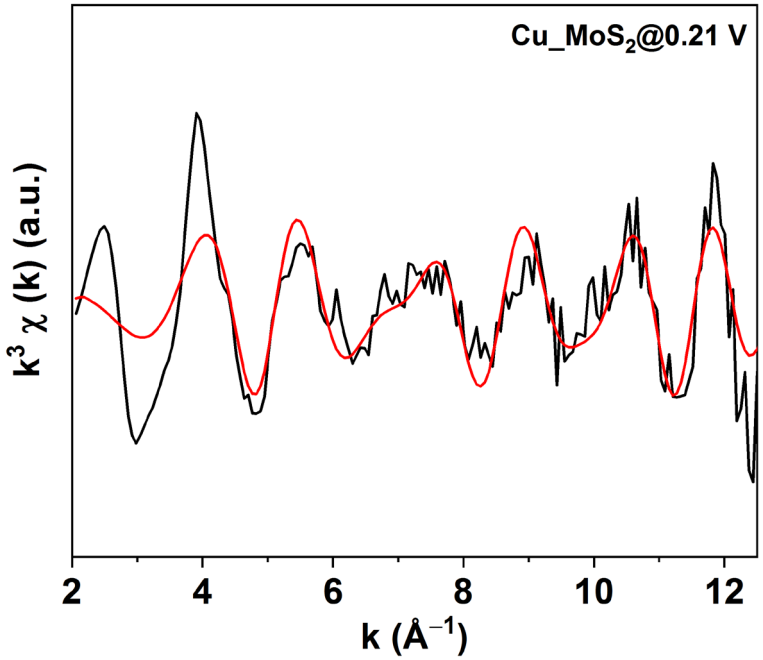

Fig. S10. Cu-K edge EXAFS spectra of Cu_MoS_2@0.21 V plotted as χ (*k*) with *k*-weight of 3. The black curve represents the experimental data and the red curve shows the Feff modeling based on the Feff R space curve fitting result.

Table S4. M-4 based R space curve fitting results.

	M-4 Model				R space curve fit	
No.	Path	Sub-model	CN[a]	R	R	± σ^2 (Å^2)
1	Cu-S(1)	M-2	2	2.36	2.37	0.0088
2	Cu-Cu	M-3	1	2.56	2.51	0.0053[c]
3	Cu-S(2)	M-3	3	2.93	2.85	0.0072
4	Cu-S(3)	M-2	2	3.27	3.39	0.0086
5	Cu-Mo(1)	M-2	1	3.46	3.39	0.0098
6	Cu-Mo(2)	M-3	1	3.87	3.95	0.0050[b]
7	Cu-Mo(3)	M-2	2	4.12	4.13	0.0100[b]

a. Fixed during R space curve fitting guided by DFT model;

b. Limit of parameter floating;

c. When CN of the Cu-Cu path is free floating, CN fit to 0.8, σ^2 fit to 0.0041.

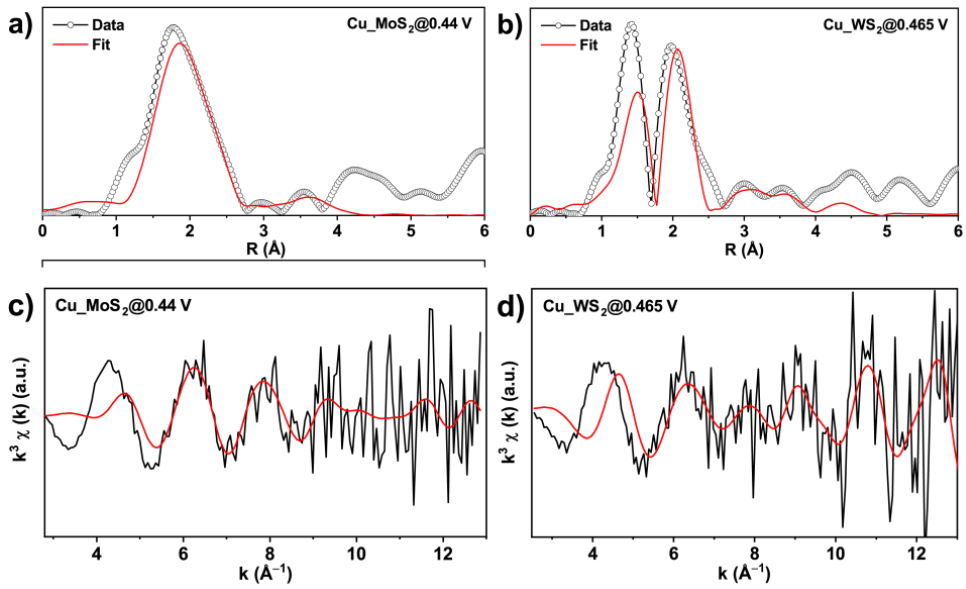

Fig. S11. Fit results corresponding to the Cu K-edge EXAFS FT spectra of Cu_MoS_2@0.44 V (a) and Cu_WS_2@0.465 V (b). Data are plotted as open circles and fits as red line; c, d) Cu-K edge EXAFS spectra of Cu_MoS_2@0.44 V (c) and Cu_WS_2@0.465 V (d) plotted as χ (*k*) with *k*-weight of 3. Black curves represent experimental data and red curves show Feff modeling based on the R space curve fitting.

Part IV: Computational Details and Results

The optimized lattice constant is 3.168 Å for the primitive cell, containing one Mo and two S atoms (Mo–S = 2.415 Å and Mo-Mo = 3.168 Å), which is in good agreement with experimental(3) and previous theoretical values.(4) The growth of metal clusters on the basal (0001) plane was modelled on a 5 x 5 supercell of MoS_2 monolayers, which leads to negligible interactions between the system and their mirror images. A vacuum region of 20 Å was added along the normal direction to the MoS_2 monolayers to avoid interactions between adjacent images. The Mo- and S-terminated edges were created by truncating MoS_2 monolayer along the $(10\bar{1}0)$ crystallographic plane, with a vacuum width of 20 Å. The Brillouin zone was sampled using a 9 × 9 × 1 Monkhorst-Pack(5) *k*-point mesh for both the basal plane and the Mo- and S-terminated edges. All structures are relaxed with fixed lattice constants until the Hellmann-Feynman force on each atom becomes smaller than 0.001 eV $Å^{-1}$.

To investigate the possible growth mode and mechanism of Cu and Cu cluster on the MoS_2, the average binding energy (E_{ab}) was calculated as follows:

$$E_{ab} = {}^{1}/_{n}\,(E_{total} - E_{subtrate} - n * E_{metal}) \quad (1)$$

where E_{total} is the total energy of the Cu-MoS_2 system, $E_{subtrate}$ is the total energy of the MoS_2 substrate, E_{metal} is the energy of the single Cu atom, and n is the number of Cu atoms. According to the above definition, a negative value of E_{ab} indicates that the process is exothermic and favourable adsorption process. To search the most stable configuration, we considered three high symmetry adsorption sites (**Fig. S15**), *i.e.*, H site (hollow site above the center of hexagons), T_{Mo} site (top site directly above a Mo atom), and T_S site (top site directly above an S atom). The E_{ab} of a single Cu atom at the H, T_{Mo}, and T_S sites are −1.63, −1.76, and −1.18 eV, respectively, indicating the most stable adsorption site of Cu atoms is the T-Mo, where the Cu atoms form 3-fold coordination with S atoms (**Fig. S16**). Cu dimer and trimer have an E_{ab} of −1.79, and −2.06 eV, respectively, with the triangular Cu-trimer found to be 0.17 eV more stable than the linearly formed Cu-trimer.

At the Mo- and S-edges, the adsorption of a single Cu atom is found to be energetically more favourable at the Mo−Mo and S−S bridge sites, respectively, as shown in **Fig. S17** and **Fig. S18**. The binding energy of a single Cu atom at the Mo-edge is calculated at −3.33 eV compared to −3.59

eV on the S-edge, suggesting that the S-edge is more active towards Cu adsorption than the Mo-edge. The stronger binding of the Cu to the MoS_2 edges than to the basal (0001) plane (E_b =−1.76 eV for single Cu atom), suggests that Cu atoms will favourably segregate to the edges rather than grow on the basal (0001) plane.

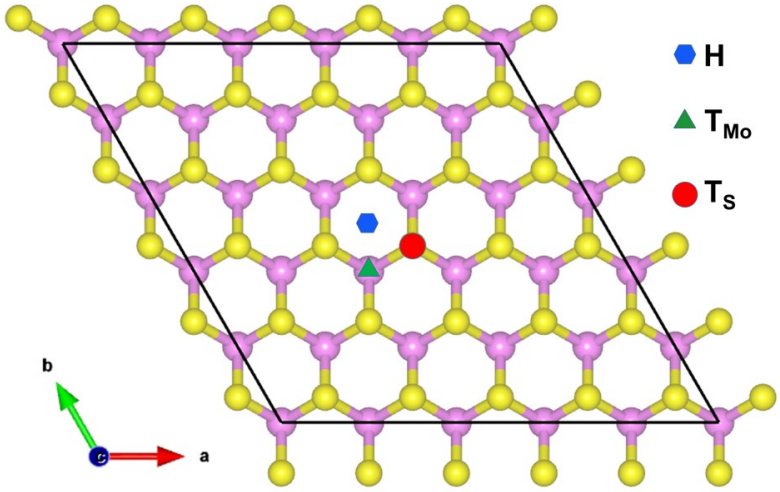

Fig. S12. Top view of (5 x 5) monolayer of MoS_2 showing the different Cu adsorption sites explored: H=hollow site above the center of hexagons, T_{Mo}=top site directly above a Mo atom, and T_S=top site directly above a S atom. Color scheme: Mo = pink and S = yellow.

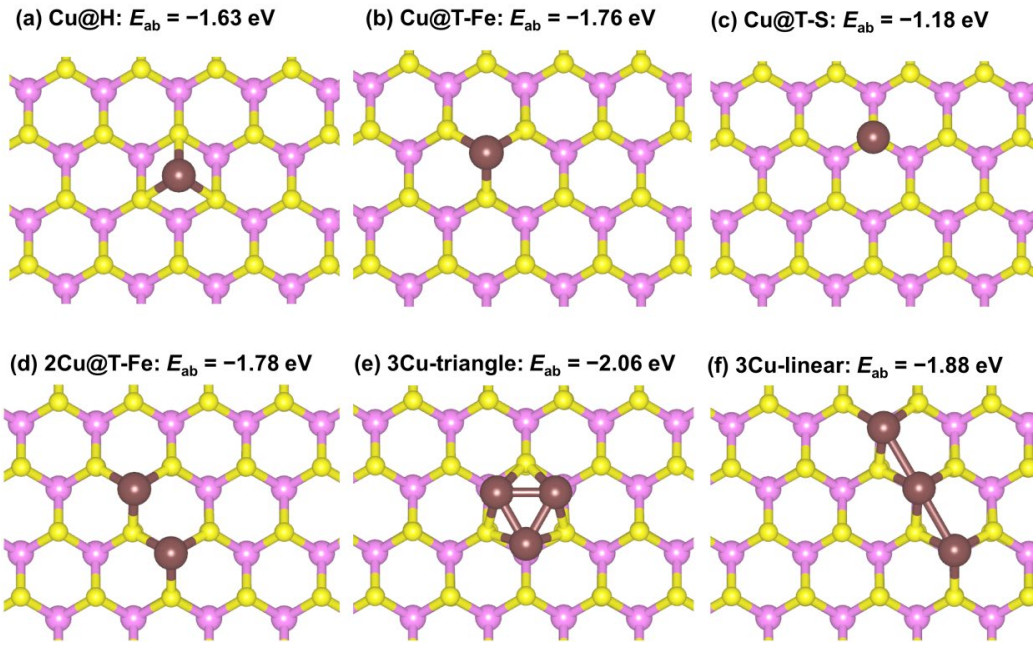

Fig. S13. Optimized structures and the average binding energies (E_{ab}) of Cu monomer, dimer, and trimer on MoS_2 basal (0001) plane. Color scheme: Mo = pink and S = yellow, Cu = brown.

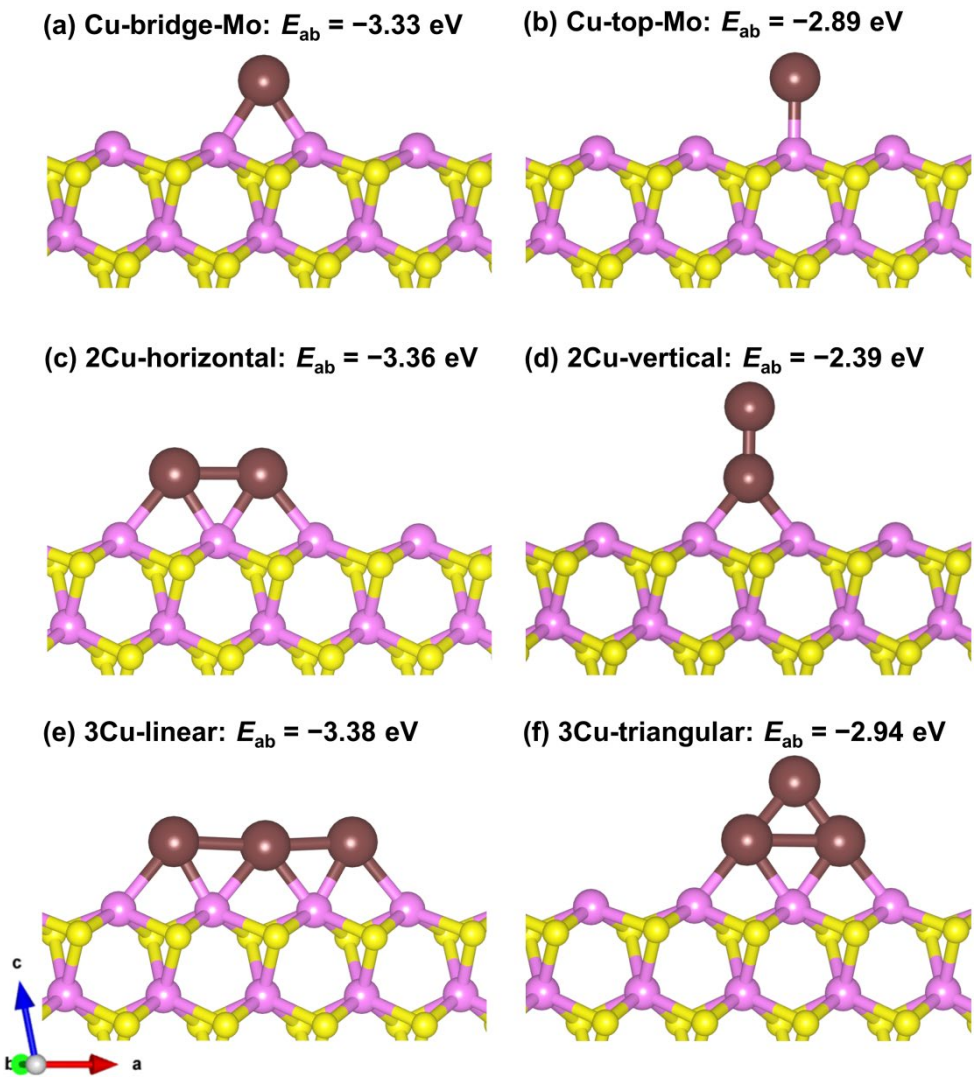

Fig. S14. Optimized structures and the average binding energies (E_{ab}) of Cu monomer, dimer, and trimer on the Mo-edge of MoS_2. Color scheme: Mo = pink and S = yellow, Cu = brown.

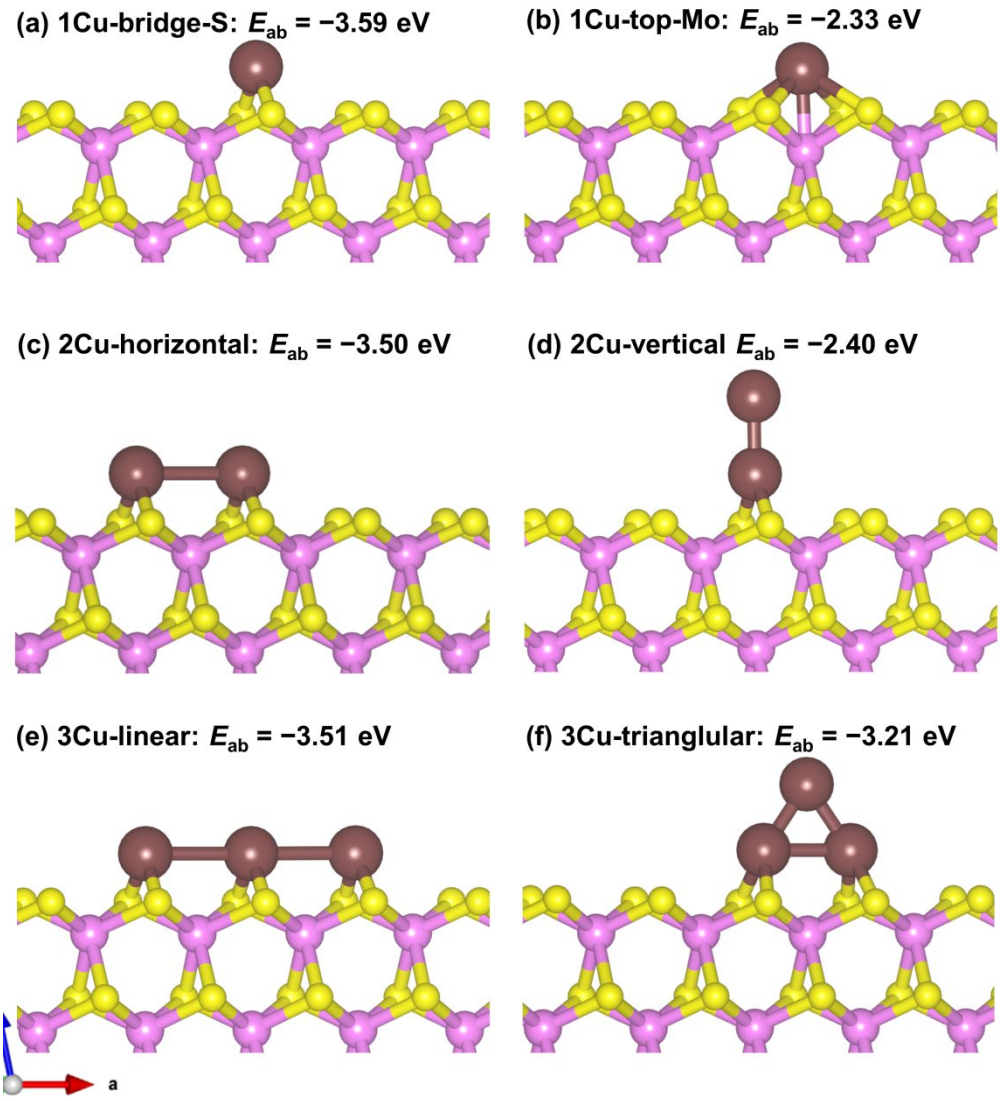

Fig. S15 Optimized structures and the average binding energies (E_{ab}) of Cu monomer, dimer, and trimer on the S-edge of MoS_2. Color scheme: Mo = pink and S = yellow, Cu = brown.

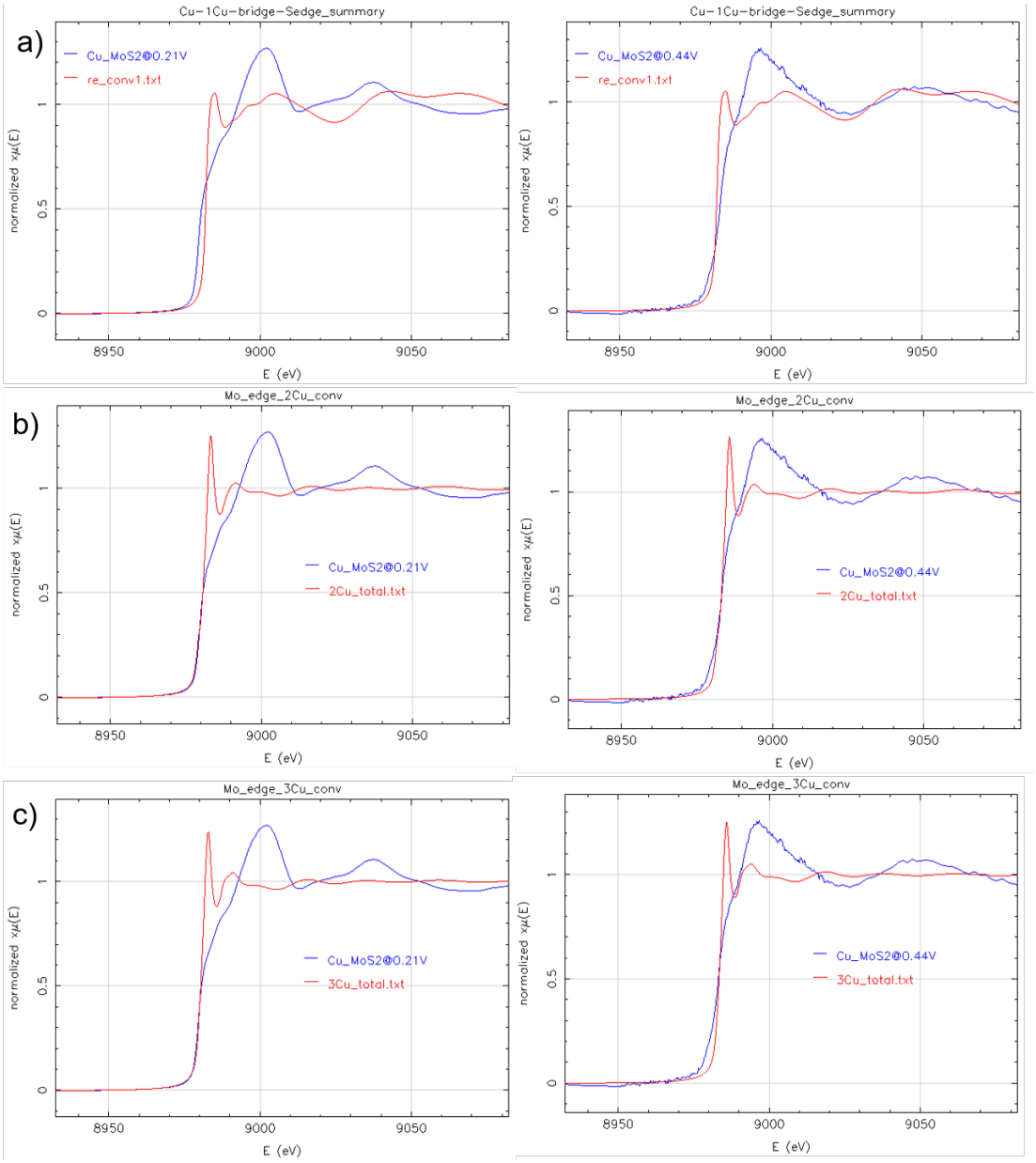

Fig. S16. Comparison between convoluted XANES (red) and experimental data (blue) based on 1Cu-bridge-S (a), 2Cu-horizontal (b) and 3Cu-linear (c) model.

References

1. A. Sharma, M. A. Verheijen, L. Wu, S. Karwal, V. Vandalon, H. C. M. Knoops, R. S. Sundaram, J. P. Hofmann, W. M. M. Kessels, A. A. Bol, *Nanoscale* **10**, 8615 (2018).

2. S. Balasubramanyam, M. Shirazi, M. A. Bloodgood, L. Wu, M. A. Verheijen, V. Vandalon, W. M. M. Kessels, J. P. Hofmann and A. A. Bol, *Chem Mater*, **31**, 5104 (2019).

3. T. Böker, R. Severin, A. Müller, C. Janowitz, R. Manzke, D. Voß, P. Krüger, A. Mazur and J. Pollmann, *Phys. Rev. B*, **64**, 235305 (2001).

4. D. Le, T. B. Rawal and T. S. Rahman, *J. Phys. Chem. C*, **118**, 5346 (2014).

5. H. J. Monkhorst and J. D. Pack, *Phys. Rev. B*, **13**, 5188 (1976).